Journal of Physics: Conference Series **512** (2014) 012021 doi:10.1088/1742-6596/512/1/012021

A note on the geometry of the quantum states of a two-level atom in external radiation fields

Marco Enríquez, Rosa Reyes and Oscar Rosas-Ortiz
Physics Department, Cinvestav, A.P. 14-740, 07000 México D.F., Mexico
E-mail: rmreyes@fis.cinvestav.mx

Abstract. We discuss some of the geometric properties of the state spaces in Quantum Mechanics with emphasis in the two-level systems case. Then the dynamics of a two-level atom affected by radiation fields is revisited in both the semiclassical and quantum approaches. In the calculations we use Hubbard operators to reduce the matrix operations into simple relations of subscripts. The time-evolution of the energy states of the atom is associated to trajectories either on the 2-sphere or in the three-dimensional unit ball according to the classical or quantum approach we are using.

1. Introduction

The geometry of state spaces is a subtle subject in quantum theories [1–6] that find applications in diverse branches of contemporary physics as the dynamical control of quantum systems [7–15] and quantum information [16], among others. Quantum states ψ cannot always be represented by vectors $|\psi\rangle$ in a Hilbert space $\mathcal{H}$ [1]; the most realistic approach uses density operators ρ to represent the state of a quantum system $\mathcal{S}$ since this last is usually prepared in a statistical ensemble of pure states $\{p_k, \psi_k\}$ better than in a given pure state ψ_r [17]. This situation provides an indication of the geometry involved since the density operator is expressed as a convex combination of orthogonal projectors $\pi_k = |\psi_k\rangle\langle\psi_k|$ that map the Hilbert space $\mathcal{H}$ into a one-dimensional subspace $\mathrm{Span}\{|\psi_k\rangle\}$ each one. The projectors can be visualized as filters characterized by certain *absorption coefficients* that are interpreted as the transition probabilities between pure states and define the geometry of the state space [1]. In this context, the pure states are represented by filters that perform the finest selection possible (*minimal filters*) and correspond to the orthogonal projectors π_k, so that the state space is the *convex hull* of all the minimal filters π_k associated to a given physical system $\mathcal{S}$. Using only vectors in a Hilbert space is not enough to represent all the possible quantum states, indeed the involved geometric structure is strongly limited in this case. It follows that "the physical reality can be too complex in order to fit in any Hilbert space" [1].

The simplest space of quantum states is associated to any two-level system (*qubit*) like the polarization of light or the spin-state of a silver atom, and this is just a three-dimensional ball of unit radius. Such a *convex body* is large enough to carry the canonical transformations that characterize the dynamics of the two-level system [1, 16]. The points on the surface (i.e. the points on the 2-sphere S^2) are in a one-to-one correspondence with the pure states of any qubit. A line segment $\overline{ab}$ connecting two arbitrary points a and b on S^2 is a convex set that represents the space of states of some classical bit whenever a and b are antipodal. Any interior point of

$\overline{ab}$ is a statistical ensemble of the pure states (*extreme points*) a and b. The entire state space of a qubit (that is, the three-dimensional ball) is therefore the intersection of all the convex sets $\overline{ab}$ that can be formed by taking arbitrary pairs $a, b \in S^2$.

Using a geometric approach the dynamics of the two-level pure states is reduced to rotations and reflections of the 2-sphere [12]. This condition is useful to determine the (classical) magnetic fields that must be applied on a spin-1/2 particle in order to control the time-evolution of its quantum state [9–11]. For instance, the particle can be compelled to evolve cyclically [9, 11] in a process that is known as *evolution loop* [7]. It is also possible to visualize experimental setups for the steering eigen-energy state to a destination without net adiabatic transitions [10]. The qubit pure states are also useful in the constructing of mesoscopic *kittens* as the appropriate linear combinations of $j = 1/2$ angular momentum eigenkets. The kittens manifest quantum interference effects analogous to those occurring for linear combinations of coherent light waves and are distinguishable by collecting them in *kitten-hoods* according to their invariance under azimuthal rotations [14].

In this communication we analyze the geometry of the state space associated with a two-level atom in external radiation fields. We shall address two different situations. A semiclassical approach is first used by considering that the energy of the atom is quantized while the field is treated as a classical entity. The state space of the entire system (atom+field) is just the 2-sphere since only qubit pure states are involved. The time-evolution of the qubit describes trajectories on S^2 that are parameterized by the field variables and can be reduced to rotations and reflections of the sphere as stated above. The population of the atom energy states is inverted in time according to the initial conditions and describes a geodesic connecting the north and south poles of S^2 (Rabi oscillations) if the atom and the field are in resonance. Non-resonant cases give rise to evolution loops that are represented as circles on the sphere. In a second step we use the quantum approach in which both the atom energies and the field are quantized. The entire system is in a pure state that is represented by vectors in the Kronecker product of the Hilbert spaces of the atom energy and field states. Here the population invertion of the atom energy states depends on the photon statistical distribution of the field: the well known Rabi oscillations are recovered for fields in a Fock state and the collapses and revivals phenomenon for fields in a Glauber state. The geometry of the atom energy states is then analyzed after the partial trace of the density operator ρ of the entire system over the field states $\rho_{at} = \mathrm{Tr}_f \rho$. At the time t, the reduced density operator $\rho_{at}(t)$ is a point of the three-dimensional ball, so that the time-evolution of the atom energy states describes trajectories in the interior of the ball.

The organization of the paper is as follows. In Section 2 we present a short survey on the geometry of quantum states by emphasizing the case of two-level systems (Section 2.1). In Section 3 we analyze the interaction between the atom and the radiation field in the X-representation. That is, we use the operators $X^{i,j}$ that cause a transition from the pure state $|\psi_j\rangle$ to the pure state $|\psi_i\rangle$ of either the atom or the field. These operators satisfy a definite set of algebraic properties and are called after Hubbard (for a recent review see [18] and references quoted therein). The X-representation reduces the matrix operations we are going to deal with into simple relations of subscripts. The well known semiclassical result of the Rabi oscillations describing the atomic transitions in time is recovered in Section 3.1. There, the atomic population invertion is connected to circles on the 2-sphere described by the time-evolution of the qubit pure states. The X-representation of the quantum treatment is given in Section 3.2; the phenomenon of collapses and revivals of the atomic transitions is recovered by assuming that the field is in a Glauber state. The analysis of $\rho_{at}(t)$ shows that the reduced state of the atom is an ensemble of pure states that describes trajectories in the interior of the three dimensional ball as it evolves in time (Section 4). We close the paper with some final remarks and conclusions.

2. A survey to the geometry of quantum states

In quantum theory the pure states ψ are represented by regular kets $|\psi\rangle$ in a Hilbert space $\mathcal{H}$. These last are vectors of finite norm ($\|\varphi\|^2 = \langle\varphi|\varphi\rangle < +\infty$) that can be normalized to unity, $\langle\varphi|\varphi\rangle = 1$. On the other hand, one of the simplest devices of measuring in quantum mechanics is a filter checking for a particle to be in a given (*idler*) state $|\varphi\rangle$. The action of the device is represented by the operator $P_\varphi = |\varphi\rangle\langle\varphi|$ producing the orthonormal projection of $\mathcal{H}$ onto the one-dimensional subspace $\mathrm{Span}\{|\varphi\rangle\} \subset \mathcal{H}$. For an arbitrary (*signal*) state $|\psi\rangle$ the action of P_φ is given by $P_\varphi|\psi\rangle = \Gamma|\varphi\rangle$, with $\Gamma = \langle\varphi|\psi\rangle \in \mathbb{C}$. Thus, the testing gives rise to one of the following results (see e.g. [2, 5]):

a) If the idler and signal kets are parallel ($|\varphi\rangle \propto |\psi\rangle$) then the answer is affirmative.
b) If the kets are orthogonal ($|\varphi\rangle \perp |\psi\rangle$), the output of the checking is negative.
c) If $|\psi\rangle = \alpha|\varphi\rangle + \beta|\eta\rangle$ with $|\varphi\rangle \perp |\eta\rangle$, the result is uncertain and depends on the coefficient $\alpha = \Gamma$. Here $|\alpha|^2 = |\langle\varphi|\psi\rangle|^2$ is the *transition probability* connected to the possibility that the system will pass the $|\varphi\rangle$-checking.

The one-dimensional space $\mathrm{Span}\{|\varphi\rangle\}$ corresponds to a whole bunch of proportional regular kets called a *ray* and denoted $[\varphi]$. Hence, the kets representing pure states are not unique since two normalized kets that differ only by a phase factor are elements of the same equivalence class

$$[\varphi] =: \{|\psi\rangle \in \mathcal{H} : |\psi\rangle = e^{i\theta}|\varphi\rangle, e^{i\theta} \in U(1)\}, \tag{1}$$

and lead to the same probabilistic predictions of the theory (i.e., $||\psi|| = ||\varphi||$) [2, 5, 14]. In general, whenever two normalized kets $|\psi_1\rangle$ and $|\psi_2\rangle$ represent two possible pure states of a system, their linear combination $|\psi\rangle = \alpha_1|\psi_1\rangle + \alpha_2|\psi_2\rangle$, with $\alpha_1, \alpha_2 \in \mathbb{C}$, represents a pure state as well.

A quantum system, however, may not be in a pure state. In practice, the quantum state of most of the physical systems is a *mixed state* ρ rather than a given pure state $|\psi\rangle \in \mathcal{H}$. The state ρ is a statistical ensemble[1] $\{p_k, \psi_k\}_{k\in\mathcal{I}}$, $\mathcal{I} \subseteq \mathbb{Z}^+$, where each pure state $|\psi_k\rangle$ occurs with probability $0 \leq p_k \leq 1$ and $\{|\psi_k\rangle\}_{k\in\mathcal{I}}$ is an orthonormal set. As a mathematical object, ρ is not a vector in the Hilbert space $\mathcal{H}$ but a linear operator $\rho : \mathcal{H} \to \mathcal{H}$ that satisfies

i) $\rho = \rho^\dagger$ (Hermiticity)
ii) $\langle\psi|\rho|\psi\rangle \geq 0$ for all $|\psi\rangle \in \mathcal{H}$ (positive definiteness)
iii) $\mathrm{Tr}\rho = 1$ (normalizability)

Thereby, the probabilities p_k and the pure states $|\psi_k\rangle$ are respectively the eigenvalues and eigenvectors of ρ which, in canonical form, is written as

$$\rho = \sum_{k\in\mathcal{I}} p_k|\psi_k\rangle\langle\psi_k|, \quad \mathcal{I} \subseteq \mathbb{Z}^+. \tag{2}$$

Assuming that we know how to prepare the pure states $|\psi_k\rangle$, we can use a classical random number generator to produce the number k with probability p_k. Every time we get a number k from the generator a copy of the system is prepared in the state $|\psi_k\rangle$. The ensemble (2) is then obtained by repeating at will such a procedure [19]. In this case p_k represents the probability

[1] We assume discrete basis for the systems we are interested in, the transition to the continuous case is straightforward.

of being prepared in the state $|\psi_k\rangle$ as well as the probability of being found in that state[2]. A mixed state ρ represents also an imprecise knowledge or inaccuracy in the preparation process of the pure states [19] (see also [20]).

Properties (ii) and (iii) give rise to the conditions

$$\sum_{k\in\mathcal{I}} p_k = 1, \quad 0 \leq p_k \leq 1. \tag{3}$$

If $p_k = 1$ for a given $k \in \mathcal{I}$ then (2) is reduced to the orthogonal projector $\rho_k := |\psi_k\rangle\langle\psi_k|$ that fulfills (i–iii) and besides is such that $\mathrm{Tr}\rho_k^2 = 1$. In this case ρ_k as well as $|\psi_k\rangle$ represent the same pure state ψ_k. Therefore, we realize that (2)–(3) correspond to a *convex combination* of the pure states ρ_k, that is,

$$\rho = \sum_{k\in\mathcal{I}} p_k\rho_k, \quad \sum_{k\in\mathcal{I}} p_k = 1, \quad 0 \leq p_k \leq 1. \tag{4}$$

In the case of a nontrivial convex combination (i.e., $0 < p_k < 1$ for at least two different values of $k \in \mathcal{I}$) one immediately shows that $\mathrm{Tr}\rho^2 < 1$. Then, for any quantum state we have

$$\mathrm{Tr}\rho^2 \leq 1, \tag{5}$$

where the equality holds only for pure states. Considering all the possible combinations (4) we see that the collection of all the density operators ρ associated to the ensemble $\{p_k, \psi_k\}_{k\in\mathcal{I}}$ is just a *convex set* with the pure states ρ_k as *extreme points*[3] [1, 3, 6, 16].

2.1. The geometry of two-level systems

Let us consider an atom with just two levels of energy. The excited $|+\rangle$ and ground $|-\rangle$ states are orthogonal

$$\langle+|+\rangle = \langle-|-\rangle = 1, \qquad \langle+|-\rangle = \langle-|+\rangle = 0, \tag{6}$$

and will be written in their simplest representation

$$|+\rangle = \begin{pmatrix} 1 \\ \\ 0 \end{pmatrix}, \qquad |-\rangle = \begin{pmatrix} 0 \\ \\ 1 \end{pmatrix}. \tag{7}$$

An arbitrary (pure) energy state of the atom $|\psi\rangle$ is then written as a normalized linear combination in the Hilbert space $\mathcal{H}_a = \mathrm{Span}\{|+\rangle, |-\rangle\}$, that is

$$|\psi\rangle = c_1|+\rangle + c_2|-\rangle, \quad |c_1|^2 + |c_2|^2 = 1, \quad c_1, c_2 \in \mathbb{C}. \tag{8}$$

The 2-tuples (7) are associated to the spectral decomposition and matrix representation of the Pauli operator σ_3 as follows

$$\sigma_3 = |+\rangle\langle+| - |-\rangle\langle-| = \begin{pmatrix} 1 & 0 \\ 0 & -1 \end{pmatrix}. \tag{9}$$

[2] In a more general situation, an arbitrary set of pure states $\{\phi_k\}_{k\in\mathcal{I}'}$ need not be orthogonal in order to define a statistical ensemble $\rho' = \{p'_k, \phi_k\}_{k\in\mathcal{I}'}$. If the kets $|\phi_k\rangle$ are not orthogonal then the probabilities p'_k of 'being prepared in' and p_k of 'being found in' the state $|\phi_k\rangle$ are not equal since, according to the point (c) indicated above, a system prepared in the state $|\phi_k\rangle$ with $k \neq \ell$ can be found (with nonzero probability) also in the state $|\phi_\ell\rangle$. Moreover, if the set $\{\phi_k\}_{k\in\mathcal{I}'}$ is not orthogonal, the probabilities p'_k are not the eigenvalues of ρ' [19].

[3] The points of a convex set that cannot be expressed as a convex combination of other points in the set are called *extreme points*.

This last together with the *creation* and *annihilation* spin-1/2 operators

$$\sigma_+ = \begin{pmatrix} 0 & 1 \\ 0 & 0 \end{pmatrix}, \quad \sigma_- = \begin{pmatrix} 0 & 0 \\ 1 & 0 \end{pmatrix}, \tag{10}$$

are the generators of the $su(2)$ Lie algebra[4]

$$[\sigma_3, \sigma_\pm] = 2\sigma_\pm, \quad [\sigma_+, \sigma_-] = \sigma_3, \tag{11}$$

and satisfy the following relations

$$\sigma_+^2 = \sigma_-^2 = 0, \quad \sigma_+^\dagger = \sigma_-, \quad \sigma_\pm|\pm\rangle = 0, \quad \sigma_\pm|\mp\rangle = |\pm\rangle. \tag{12}$$

In this representation the observable of the energy is the Hamiltonian

$$H_a = \frac{1}{2}\hbar\omega_a\sigma_3, \tag{13}$$

with ω_a the atomic transition frequency. Another observable of interest is the density operator ρ which in the representation (9) acquires the general form

$$\rho = \begin{pmatrix} \rho_{11} & \rho_{12} \\ \\ \rho_{21} & \rho_{22} \end{pmatrix} = \frac{1}{2}\left(\mathbb{I} + \vec{\tau}\cdot\vec{\sigma}\right), \quad \vec{\tau} = (\tau_1, \tau_2, \tau_3), \quad \vec{\sigma} = (\sigma_1, \sigma_2, \sigma_3). \tag{14}$$

Indeed, this operator is (i) Hermitian if $\rho_{11}, \rho_{22} \in \mathbb{R}$ and $\rho_{12} = \overline{\rho}_{21}$ (ii) definite positive if $|\rho_{12}| = |\rho_{21}| \leq \sqrt{\rho_{11}\rho_{22}}$, and (iii) normalized if $\rho_{11} + \rho_{22} = 1$. Considering these three properties one can verify that the elements of the *Bloch vector* $\vec{\tau}$ satisfy the equation of a three-dimensional ball of unit radius $B[0, 1]$,

$$\mathrm{Tr}\rho_a^2 = \tau_1^2 + \tau_2^2 + \tau_3^2 \leq 1, \tag{15}$$

and are given by

$$\tau_1 = \rho_{12} + \rho_{21} = 2\mathrm{Re}(\rho_{12}), \quad \tau_2 = i(\rho_{12} - \rho_{21}) = 2\mathrm{Im}(\rho_{12}), \quad \tau_3 = \rho_{11} - \rho_{22}. \tag{16}$$

It is illustrative to notice that the Bloch vector $\vec{\tau}$ is also associated to the expectation value of $\vec{\sigma}$ calculated in the basis of pure states $|\pm\rangle$; namely $\tau_k = \langle\sigma_k\rangle = \mathrm{Tr}(\rho\sigma_k)$ for $k = 1, 2, 3$. Thus, $\mathbf{n} = \langle\vec{\sigma}\rangle = \mathrm{Tr}(\rho\vec{\sigma})$ is a point on the 2-sphere $S^2 \subset B[0, 1]$ since $\vec{\tau} = \mathbf{n}$ in Eq. (15) is in this case such that $||\mathbf{n}|| = 1$. This representation of the energy pure states of the two-level atom leads to a fibre-bundle formulation of the qubit dynamics. The *Hopf fibring* [21] (see also [22]) of the 3-sphere S^3 over the base space S^2 with fibre S^1 yields the geometry of qubit pure states

$$S^1 - S^3 \xrightarrow{\pi} S^2.$$

Equations (16) correspond to the *Hopf mapping* π, the 3-sphere is the space of rays (1) belonging to the 2-dimensional Hilbert space $\mathcal{H}_a = \mathrm{Span}\{|+\rangle, |-\rangle\}$, and the fibre S^1 defines the rays in terms of the phases $e^{i\theta} \in U(1)$. All the points on S^2 represent energy pure states of the atom, any inner point of $B[0, 1]$, on the other hand, represents a mixed state of $|\pm\rangle$.

[4] In terms of the Pauli matrices σ_3, $\sigma_1 = \sigma_+ + \sigma_-$, and $\sigma_2 = i(\sigma_- - \sigma_+)$, the $su(2)$ algebra reads $[\sigma_i, \sigma_j] = 2\epsilon_{ijk}\sigma_k$, where $i, j, k = 1, 2, 3$ and ϵ_{ijk} is the total anti-symmetric Levi-Civita tensor.

3. Atom-Field interaction

In this section we are interested in the interaction between a two-level atom and a radiation field. To simplify the calculations we shall use the X-representation of operators that is obtained by considering the Hubbard operators in their simplest form [18]. That is, we shall use n-square matrices $X^{i,j}$ which have entry 1 in position (i,j) and zero in all other entries at the time that they fulfill the multiplication rule

$$X^{i,j}X^{k,m} = \delta_{jk}X^{i,m}, \tag{17}$$

and have the properties

$$(X^{i,j})^\dagger = X^{j,i}, \quad \sum_k X^{k,k} = \mathbb{I}, \quad [X^{i,j}, X^{k,m}]_\pm = \delta_{jk}X^{i,m} \pm \delta_{mi}X^{k,j}, \tag{18}$$

with $\mathbb{I}$ the identity matrix and $[A,B]_\pm$ standing for either the commutator $(-)$ or the anticommutator $(+)$ of A and B.

In X-representation any operator A acting on $\mathcal{H}_a = \mathrm{Span}\{|+\rangle, |-\rangle\}$ is expressed as a linear combination

$$A = \sum_{k,j=1}^{2} a_{k,j}X^{i,j}, \quad a_{k,j} \in \mathbb{C}, \tag{19}$$

where the coefficients $a_{k,j}$ are defined accordingly. For instance, the $su(2)$ generators (9) and (10) read as

$$\sigma_3 = X^{1,1} - X^{2,2}, \quad \sigma_+ = X^{1,2}, \quad \sigma_- = X^{2,1}, \tag{20}$$

while the Hamiltonian (13) and the identity $\mathbb{I}_2$ are written in the form

$$H_a = \frac{1}{2}\hbar\omega_a(X^{1,1} - X^{2,2}), \quad \mathbb{I}_2 = X^{1,1} + X^{2,2}. \tag{21}$$

3.1. Classical fields

As a first approach let us consider the situation in which the (electric) radiation field can be described in a purely classical manner. Considering the case of single mode we have

$$\vec{E}(t) = \mathcal{E}\left(e^{-i\omega_f t} + e^{i\omega_f t}\right)\mathbf{e}_f. \tag{22}$$

Here $\mathcal{E}$, ω_f and $\mathbf{e}_f$ are respectively the amplitude, the frequency and the polarization of the field. The most general form of the interaction Hamiltonian H_{Icl} is in this case given by

$$H_{Icl} = \sum_{k,j=1}^{2} \lambda_{k,j}X^{i,j}. \tag{23}$$

The coefficients $\lambda_{i,j}$ of this last combination are characterized by the field parameters [23, 24]. Using the dipole approximation one immediately gets $\lambda_{1,1} = \lambda_{2,2} = 0$ and $\lambda_{1,2} = \lambda_{2,1} = 2\hbar\gamma\cos(\omega_f t)$, where $\gamma = (\frac{p}{\hbar}\mathcal{E})\mathbf{e}_f \cdot \mathbf{e}_p$ stands for the classical *Rabi frequency* and p, $\mathbf{e}_p$, are respectively the "size" and orientation of the atom dipole momentum $\vec{p}$ that defines the approximation. From (20) the interaction Hamiltonian (23) acquires the usual form

$$H_{Icl} = \hbar\gamma(\sigma_+ + \sigma_-). \tag{24}$$

Now we use the Hamiltonian (13) to introduce a rotating frame description by means of the unitary transformation

$$|\psi\rangle_R = e^{iH_a t/\hbar}|\psi\rangle. \tag{25}$$

Then H_a is invariant under such a transformation while H_{Icl} is mapped into the expression

$$\widetilde{H}_{Icl} = H_{Icl} + 2\hbar\gamma(\sigma_+ e^{i2\omega_f t})_{sim}, \tag{26}$$

with $A_{sim} = (A + A^\dagger)/2$. In the rotating wave approximation we can omit the second term in the last expression so that $\widetilde{H}_{Icl} = H_{Icl}$. Finally, let us take $\frac{\hbar}{2}\omega_f$ and $\hbar\omega_a$ respectively as the zero and unit of energy to write the Hamiltonian of the entire system (atom+field) in the conventional form (see e.g. [23–26]):

$$H_{cl} = H_a + H_{Icl} = \frac{\Delta}{2}\sigma_3 + g(\sigma_+ + \sigma_-), \qquad \Delta = 1 - \frac{\omega_f}{\omega_a}, \quad g = \frac{\gamma}{\omega_a}. \tag{27}$$

The (dimensionless) parameter Δ stands for the *detuning* between the radiation field and the atomic transition. The time-evolution operator $U_{cl}(t) = e^{iH_{cl}t}$ is easily achieved

$$U_{cl}(t) = c_+(t)X^{1,1} + c_+^*(t)X^{2,2} + 2\left(c_-^*(t)X^{1,2}\right)_{sim} \tag{28}$$

where z^* is the complex conjugate of $z \in \mathbb{C}$ and

$$c_+(t) = \cos\Omega t - i\frac{\Delta}{2\Omega}\sin\Omega t, \qquad c_-(t) = i\frac{g}{\Omega}\sin\Omega t, \tag{29}$$

with $\Omega = \sqrt{\Delta^2/4 + g^2}$ a generalized Rabi frequency (this is reduced to the usual Rabi frequency when $\Delta = 0$). To get some insights on the time-evolution of the system let us assume that the atom is initially in the pure state $|\psi(0)\rangle_R = |+\rangle$. One gets

$$|\psi(t)\rangle_R = U(t)|\psi(0)\rangle_R = c_+(t)|+\rangle + c_-(t)|-\rangle, \tag{30}$$

so that the atomic population is inverted according to the rule

$$\langle\sigma_3(t)\rangle = |c_+(t)|^2 - |c_-(t)|^2 = \left(\frac{g}{\Omega}\right)^2\cos(2\Omega t) + \left(\frac{\Delta}{2\Omega}\right)^2. \tag{31}$$

At resonance ($\Delta = 0$) the well known Rabi oscillations between $|+\rangle$ and $|-\rangle$ are recovered

$$\langle\sigma_3(t)\rangle = \cos(2gt). \tag{32}$$

Figure 1 shows the behavior of (31) for different values of the detuning. If $\Delta = 0$ the atomic population is inverted from $|+\rangle$ to $|-\rangle$ and vice versa at the (dimensionless) Rabi frequency $g = \gamma/\omega_a$. Out of resonance ($\Delta \neq 0$) the initial atomic population $|c_+(t)|^2$ periodically decreases its value and recovers this at the generalized Rabi frequency Ω. In this case $|c_+(t)|^2$ is never zero so that the atom is not able to arrive at the state $|-\rangle$ in any time. Indeed this evolves from $|+\rangle$ to a linear superposition of $|+\rangle$ and $|-\rangle$, and after a while determined by Ω the atom goes back to the state $|+\rangle$ (see the cases $\Delta = g$ and $\Delta = 4g$ in Figure 1).

The pure state (30) can be represented also by a projector with the properties i)–iii) of a density operator we have discussed in the previous section, this reads as

$$\rho(t) = |\psi(t)\rangle\langle\psi(t)| = |c_+|^2X^{1,1} + |c_-|^2X^{2,2} + 2\left(c_+\overline{c}_-X^{1,2}\right)_{sim}, \tag{33}$$

where the time-dependence of the coefficients has been assumed as implicit. The Bloch vector associated to the state (33) is normalized ($\vec{\tau} = \mathbf{n}$) and evolves in time by describing a trajectory on the 2-sphere S^2 that is parameterized as follows

$$\begin{gathered} n_1(t) = 2\mathrm{Re}(c_+\overline{c}_-) = -\frac{g\Delta}{\Omega^2}\sin^2(\Omega t), \quad n_2(t) = 2\mathrm{Im}(c_+\overline{c}_-) = -\frac{g}{\Omega}\sin(2\Omega t), \\ n_3(t) = |c_+|^2 - |c_-|^2 = \left(\frac{g}{\Omega}\right)^2\cos(2\Omega t) + \left(\frac{\Delta}{2\Omega}\right)^2. \end{gathered} \tag{34}$$

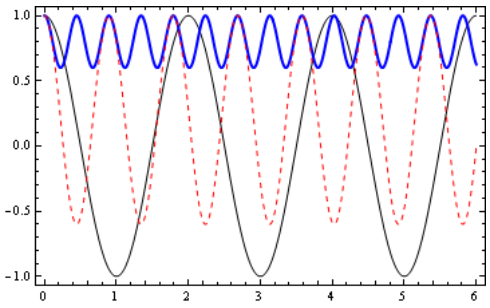

Figure 1. The atomic population invertion obtained in the semiclassical approach (31). If the atomic transitions are in resonance with the field (black curve) one recovers the well known Rabi oscillations between $|+\rangle$ and $|-\rangle$. For other values of the detuning ($\Delta = g$ in red, $\Delta = 4g$ in blue) an atom in the initial state $|+\rangle$ has not the possibility to evolve into $|-\rangle$ with certainty.

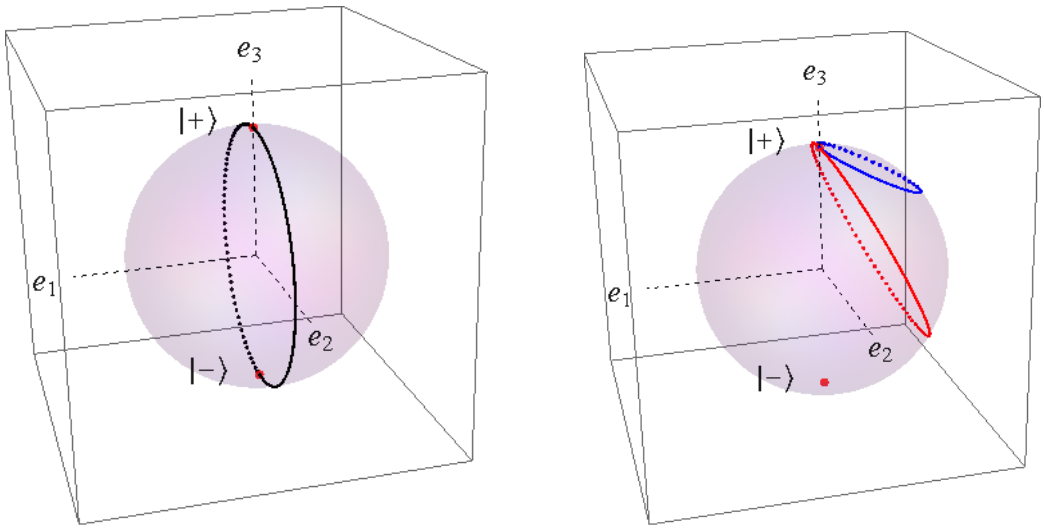

Figure 2. In the semiclassical approach the state space of an atom in a single mode radiation field is just a 2-sphere because only the pure states of the atom are involved. At resonance, the qubit describes a geodesic on the yz-plane (left) while other values of the detuning give rise to circles on the sphere that have the north pole as common point. The paths for $\Delta = g$ (red) and $\Delta = 4g$ (blue) have been depicted here (right) for comparison with Figure 1. In all cases the north pole is the initial state and the system comes back to this point in a period $T_n = n\pi/\Omega, n \in \mathbb{Z}$.

In general, the Bloch vector $\mathbf{n}$ describes circles on S^2 that pass over the north pole (N) periodically in time; the greater the value of Δ the smaller the diameter of the circle (see Figure 2). The points P integrating these circles are connected to N by a chord $\overline{NP}$ that fulfills $0 \leq \overline{NP} \leq 2$, with 2 the diameter of the 2-sphere. Such paths are also the geometric representation of the atomic population invertion (31) as this evolves in time. At resonance $\Delta = 0$, the circle corresponds to a geodesic passing over the south pole (S) in the yz-plane. In the vicinity of resonance the circles are defined over a plane which is almost parallel to the yz-one and pass over points that are close to the south pole. Thus, the atom evolves from $|+\rangle$ to a linear superposition (30) that is dominated by $|-\rangle$ at a half a period $T/2 = \frac{\pi}{2\Omega} \approx \frac{\pi}{4g}$ for $\Delta \approx 0$. Other values of Δ produce different linear superpositions at $T/2$. For instance, in Figure 2 we

see that the chord $\overline{NP}$ defined by the points P belonging to the circle for $\Delta = 2g$ is smaller than the chord obtained for $\Delta = g/2$. This means that the influence of $|+\rangle$ in the superposition (30) increases as the value of Δ. For arbitrary initial states written as the linear superposition of the north and south poles the trajectories are the same as those described above. This is just necessary to consider that any point on the sphere can be transformed into N, and vice versa, by the appropriate set of rigid rotations.

3.2. quantized fields

If the description of the radiation field requires the inclusion of quantum properties then the electric vector (22) is substituted by the vectorial operator

$$\vec{\hat{E}}(t) = \mathcal{E}\left(\hat{a}e^{-i\omega_f t} + \hat{a}^\dagger e^{i\omega_f t}\right)\mathbf{e}_f, \tag{35}$$

where $\hat{a}$ and $\hat{a}^\dagger$ are the boson annihilation and creation operators fulfilling the photon algebra

$$[\hat{a}, \hat{a}^\dagger] = \mathbb{I}_f, \quad [\hat{N}, \hat{a}] = -\hat{a}, \quad [\hat{N}, \hat{a}^\dagger] = \hat{a}^\dagger, \tag{36}$$

with $\hat{N} = \hat{a}^\dagger\hat{a}$ the number operator and $\mathbb{I}_f$ the identity operator in the Hilbert space $\mathcal{H}_f = \text{Span}\{|n\rangle\}_{n\in\mathbb{Z}^+}$. The action of the above operators on the Fock vectors $|n\rangle$, $n \in \mathbb{Z}^+$, is as follows

$$\hat{a}|n\rangle = \sqrt{n}|n-1\rangle, \quad \hat{a}^\dagger|n\rangle = \sqrt{n+1}|n+1\rangle, \quad \hat{N}|n\rangle = n|n\rangle. \tag{37}$$

For simplicity we shall omit the "hat" in the representing of operators ($\hat{A} \leftrightarrow A$) while we use the number 1 instead of $\mathbb{I}_f$ whenever there will be no confusion in notation. The Hamiltonian of the field is in the Fock's representation given by

$$H_f = \hbar\omega_f\left(N + \frac{1}{2}\right), \tag{38}$$

so that $H_f|n\rangle = \hbar\omega_f(n + \frac{1}{2})|n\rangle$. Thus, $\mathcal{H}_f$ is the state space spanned by the energy eigenvectors of the field. The entire quantum system $\mathcal{S} = \mathcal{S}_a + \mathcal{S}_f$ is a composite of the atom $\mathcal{S}_a$ and the field $\mathcal{S}_f$, so that the energy observables (21) and (38) should be promoted to act on the state space of $\mathcal{S}$. We have

$$H_a \to H_a \otimes \mathbb{I}_f, \qquad H_f \to \mathbb{I}_2 \otimes H_f, \tag{39}$$

with $\otimes$ the Kronecker product of operators [18]. Then H_a and H_f are the energy observables of the atom alone and the field alone. Accordingly, the free of interaction Hamiltonian reads as

$$H_0 = H_a \otimes \mathbb{I}_f + \mathbb{I}_a \otimes H_f = \begin{pmatrix} \frac{\hbar\omega_a}{2}\Delta + \hbar\omega_f(N+1) & 0 \\ 0 & -\frac{\hbar\omega_a}{2}\Delta + \hbar\omega_f N \end{pmatrix}. \tag{40}$$

Notice that the matrix elements of H_0 are in the Fock's representation. The eigenvectors and eigenvalues of this operator are defined as follows

$$\begin{aligned} H_0|+,n\rangle &= \hbar\left[\omega_f(n+1) + \tfrac{\omega_a}{2}\Delta\right]|+,n\rangle, \\ H_0|-,n+1\rangle &= \hbar\left[\omega_f(n+1) - \tfrac{\omega_a}{2}\Delta\right]|-,n+1\rangle, \end{aligned} \tag{41}$$

where

$$|+,n\rangle \equiv |+\rangle \otimes |n\rangle = \begin{pmatrix} |n\rangle \\ |\emptyset\rangle \end{pmatrix}, \quad |-,n+1\rangle \equiv |-\rangle \otimes |n+1\rangle = \begin{pmatrix} |\emptyset\rangle \\ |n+1\rangle \end{pmatrix}, \tag{42}$$

with $|\emptyset\rangle$ the null vector in $\mathcal{H}_f$. If the interaction between the atom and the field is considered then, in a first approximation, we can write

$$H_I = \sum_{i,j=1}^{2} \sum_{k,\ell=0}^{+\infty} \lambda_{i,j;k,\ell} X^{i,j} \otimes X_f^{k,\ell}, \tag{43}$$

where $X_f^{k,\ell}$ is an infinite square matrix that has entry 1 in position (k,ℓ) and zero in all other entries [18]. This last kind of matrices is useful in the constructing of the X-representation of the boson operators [23, 24]:

$$a = \sqrt{N} \sum_{n=0}^{+\infty} X_f^{n,n+1}, \quad a^\dagger = \sqrt{N} \sum_{n=0}^{+\infty} X_f^{n+1,n}. \tag{44}$$

Using the same approximations as in Section 3.1 one arrives at the simplest form of the interaction Hamiltonian

$$H_I = \gamma(\sigma_+ \otimes a + \sigma_- \otimes a^\dagger) = \begin{pmatrix} 0 & \gamma a \\ \gamma a^\dagger & 0 \end{pmatrix}. \tag{45}$$

Therefore, the Hamiltonian of the entire system in the rotating frame is just the one appearing in the Jaynes-Cummings model [27] (see also [28]):

$$H = \frac{\Delta}{2} \sigma_3 \otimes \mathbb{I}_f + H_I, \tag{46}$$

where $\hbar\omega_f/2$ and $\hbar\omega_a$ are respectively the zero and the unit of the energy. The time-evolution operator is in this case [18, 23, 24]:

$$U(t) = e^{iHt} = C_+(N+1,t) X^{1,1} + C_+^\dagger(N,t) X^{2,2} + 2 \left(C_-^\dagger(N,t) X^{1,2} \right)_{sim} \tag{47}$$

where the operators $C_\pm(N,t)$ are defined in the Fock's representation

$$C_+(N,t) = \cos(\Omega_N t) - \frac{i\Delta}{2\Omega_N} \sin(\Omega_N t), \quad C_-(N,t) = a^\dagger \left(\frac{ig}{\Omega_{N+1}} \right) \sin(\Omega_{N+1} t), \tag{48}$$

with $\Omega_N = \sqrt{\Delta^2/4 + gN}$. Thus, they act on the number states $|n\rangle$ as follows

$$C_+(N,t)|n\rangle = c_+(n,t)|n\rangle, \quad C_-(N,t)|n\rangle = c_-(n,t)|n+1\rangle. \tag{49}$$

The $c_\pm(n,t)$ functions are given by

$$c_+(n,t) = \cos(\Omega_n t) - \frac{i\Delta}{2\Omega_n} \sin(\Omega_n t), \quad c_-(n,t) = \sqrt{n+1} \left(\frac{ig}{\Omega_{n+1}} \right) \sin(\Omega_{n+1} t). \tag{50}$$

Let us assume that $|\psi(0)\rangle_R = |+,n\rangle$ is the initial sate of the entire system. The time-evolved state is then of the form

$$|\psi(t)\rangle_R = U(t)|\psi(0)\rangle_R = c_+(n+1,t)|+,n\rangle + c_-(n,t)|-,n+1\rangle, \tag{51}$$

and the atomic population invertion as a function of time is

$$\langle\sigma(t)\rangle_n = \left(\frac{g\sqrt{n+1}}{\Omega_{n+1}} \right)^2 \cos(2\Omega_{n+1} t) + \left(\frac{\Delta}{2\Omega_{n+1}} \right)^2. \tag{52}$$

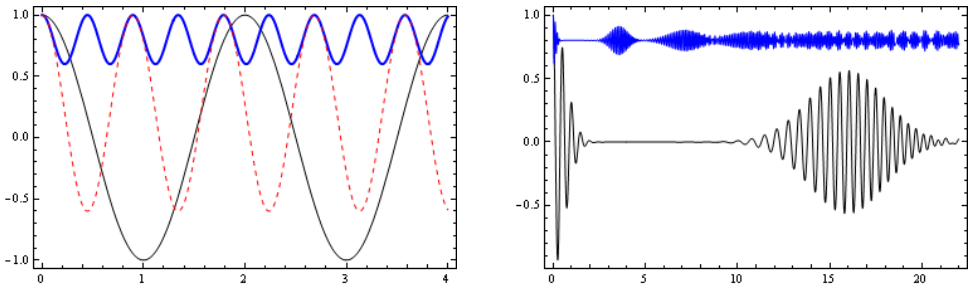

Figure 3. The atomic population invertion obtained in the quantum approach for the field in the Fock state $|n\rangle$ (Eq. (52), left) and in the Glauber state with $\overline{n} = 15$ (Eq. (56), right) for different values of the detuning ($\Delta = 0$ in black, $\Delta = g$ in red and $\Delta = 4g$ in blue).

In Figure 3 we can see the dependence of the population invertion (52) on the detuning Δ. At resonance ($\Delta = 0$) the atomic population oscillates in time from $|+\rangle$ to $|-\rangle$ while the field transits from the Fock state $|n\rangle$ to $|n+1\rangle$ at the frequency Ω_n (notice this occurs even for the zero photons $n = 0$ case, as expected). The situation illustrated in Figure 3 is quite similar to that presented in Figure 1 (except in the zero photons case) because in both cases we have analyzed the time-evolution of the pure states of the atom+field system. In the quantum approach this is given by the Kronecker product state $|+, n\rangle$ while in the classical approach we have the simple pure state $|+\rangle$. In the next section we shall discuss on the main differences between the semiclassical and the quantum approaches when one looks for the dynamics of the atom states alone.

If the field is not in a definite state of the energy one can consider the initial state

$$|\psi(0)\rangle = \sum_{k=0}^{\infty} \alpha_k |+, k\rangle, \quad \text{with} \quad \sum_{k=0}^{\infty} |\alpha_k|^2 = 1. \tag{53}$$

The atomic population invertion is in this case

$$\langle \sigma_3 \rangle = \sum_{k=0}^{\infty} |\alpha_k|^2 \langle \sigma_3 \rangle_k. \tag{54}$$

For instance, if (53) is a Glauber state then

$$|\alpha_k|^2 = \frac{e^{-\overline{n}}\ \overline{n}^k}{k!}, \qquad \overline{n} = |\alpha|^2, \quad \alpha \in \mathbb{C}, \tag{55}$$

with $\overline{n}$ standing for the mean photon number. At resonance the atomic population invertion (54) yields

$$\langle \sigma_3 \rangle = e^{-\overline{n}} \sum_{k=0}^{\infty} \frac{e^{-\overline{n}}\ \overline{n}^k}{k!} \cos(2gt). \tag{56}$$

The Figure 3 shows the behavior of the atomic population invertion in the cases (52) and (56) for different values of the involved parameters. There, we can appreciate that the time evolution of the atom energy states depends on the statistical distribution of the photons that integrate the radiation bath. The collapses and revivals phenomenon is a direct consequence of the classical properties associated to the Glauber quantum states.

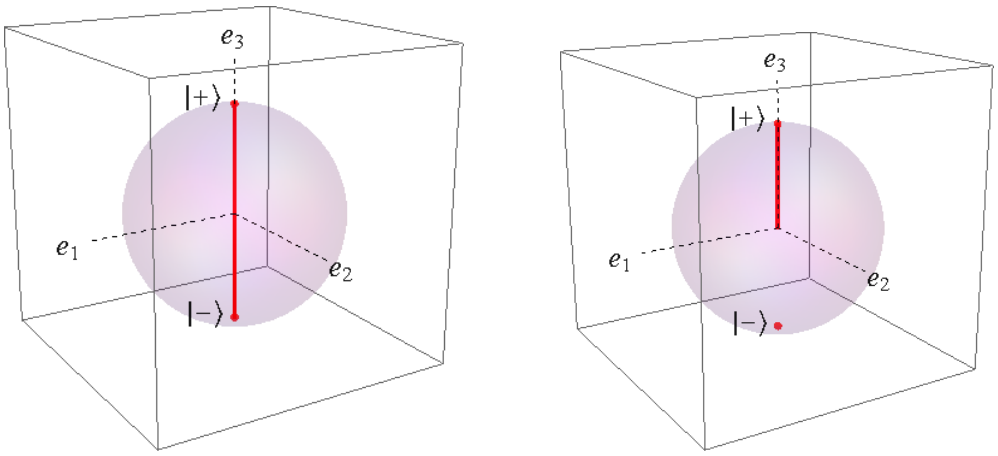

Figure 4. If the atom is initially in the energy state $|+\rangle$ and the field in the Fock state $|n\rangle$ then the entire system (atom+field) is in the pure state (51) and describes the time-evolution presented in Figure 3. If one focuses on the atomic part only, then the reduced state ρ_c in (57) describes the segment lines illustrated at the left for $\Delta = 0$ and at the right for $\Delta = 2g\sqrt{n+1}$ and $n = 2$. Notice that in this last case the total chaos $(0, 0, 0)$ is a part of the involved segment line.

4. Mixed states

The pure state (51) can be represented also by the projector $\rho(t) = |\psi(t)\rangle_R\langle\psi(t)|$, which is the density operator associated to the entire system and fulfills $\mathrm{Tr}\rho^2(t) = 1$. We are interested in the description of the atom alone, so that we use the partial trace over the field states to get

$$\rho_a(t) = \mathrm{Tr}_f\rho(t) = |c_+(n+1,t)|^2 X^{1,1} + |c_-(n,t)|^2 X^{2,2}. \tag{57}$$

This last operator is such that $\mathrm{Tr}\rho_a^2(t) \leq 1$. Therefore (57) is the mixed state associated to the ensemble of pure states $X^{1,1} \leftrightarrow |+\rangle$ and $X^{2,2} \leftrightarrow |-\rangle$, with probabilities $|c_+(n+1,t)|^2$ and $|c_-(n,t)|^2$ respectively. Moreover, $\rho_a(t)$ defines a convex set which is just the chord connecting the north and the south poles of the three-dimensional unit ball (see Figure 4). This assertion is verified by calculating the Bloch vector $\vec{\tau}$, one finds that only the third component is different from zero,

$$\tau_3 = \left(\frac{g\sqrt{n+1}}{\Omega_{n+1}}\right)^2 \cos(2\Omega_{n+1}t) + \left(\frac{\Delta}{2\Omega_{n+1}}\right)^2. \tag{58}$$

The parametrization(58) describes a segment of line on the z-axis which is contained in the chord $\overline{NS}$ connecting any of the circles passing over the north and the south poles of $B[0,1]$. At resonance the segment of line is just $\overline{NS}$. The point of "total chaos" $(0,0,0)$ is reached whenever

$$\cos(2\Omega_{n+1}t) = -\frac{\Delta^2}{4g^2(n+1)}, \tag{59}$$

is fulfilled, so that $\Delta \leq 2g\sqrt{n+1}$ (in Figure 4 we show the case when the identity of this last expression is fulfilled with $n = 2$).

For arbitrary states of the field energy (53) the atom state is off-diagonal

$$\rho_a = \sum_{ij=1}^{2} \rho_{ij} X^{i,j}, \tag{60}$$

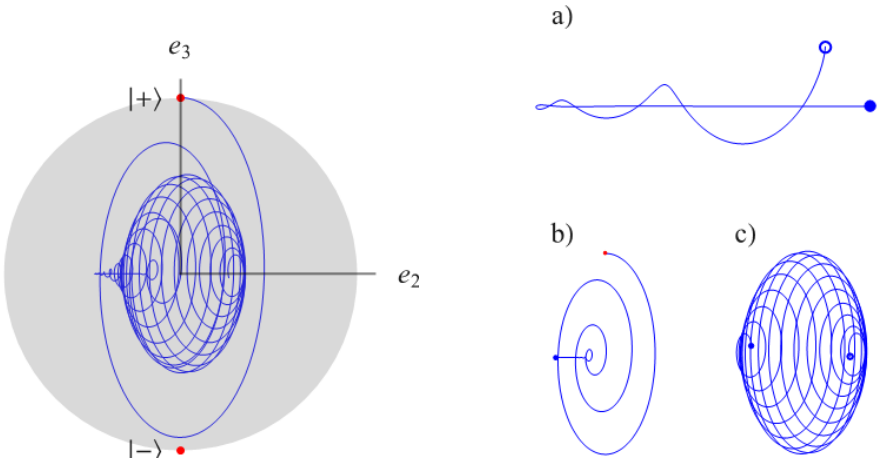

Figure 5. If the atom is in the initial state $|+\rangle$ and the field is in a Glauber state (55) the atomic reduced state ρ_c describes trajectories in the interior of the three-dimensional ball (left). The plot is at resonance with $\overline{n} = 15$. The time-evolution depicted here is in the interval $[0, 9.9\pi]$, in Ω units. At the right we show the partial intervals (b) $[0, 4\pi]$ (a) $[2.6\pi, 5\pi]$ and (c) $[6\pi, 9.9\pi]$, in all cases a red disk means pure state, a blue circle is for initial state and a blue disk denotes final state. All the path is described on the disk defined by the intersection of the yz-plane and the ball $B[0, 1]$.

with coefficients (the time dependence is implicit)

$$\rho_{11} = \sum_{k=0}^{+\infty} |\alpha_k \, c_+(k{+}1)|^2, \quad \rho_{12} = \rho_{21}^* = \sum_{k=0}^{+\infty} \alpha_{k+1}\alpha_k^* \, c_+(k{+}2) \, c_-^*(k), \quad \rho_{22} = \sum_{k=0}^{+\infty} |\alpha_k \, c_-(k)|^2. \quad (61)$$

Using (16) we can evaluate the trajectories described by the Bloch vector in the three-dimensional unit ball. The Figure 5 shows the situation obtained when the atom is initially in the pure state $|+\rangle$ and the field is in a (pure) Glauber state defined by $\overline{n} = 15$. There, we can see that the atom state departures from the north pole of the ball (pure state $|+\rangle$) at $t = 0$ and goes inside that convex body for arbitrary values of $t \neq 0$. In the picture we have assumed that the atomic transitions and the field are in resonance so that all the path is depicted in the disk defined by the intersection of the yz-plane and the ball $B[0, 1]$. Other values of the detuning $\Delta \neq 0$ give rise to paths that are more elaborated in the interior of the ball. Similar results can be found in [28].

5. Conclusions

We have studied the interaction of a single qubit with a single mode radiation field both in the semiclassical and quantum approaches. The geometry of the related state space has been discussed and the time-evolution of the energy states of the atom are found to describe trajectories in the three-dimensional ball of unit radius. In the semiclassical treatment only the pure states $|\pm\rangle$ of the atomic energy are involved so the geometric representation is on the points of the 2-sphere. At resonance with the radiation bath the energy state of the atom describes a geodesic on the yz-plane that passes over the north and the south poles. For other values of the detuning Δ, the paths followed by the energy state are circles over the sphere that has the north pole as common point. In the quantum case we have shown that the entire system (atom+field)

is in a pure state that evolves in time depending on the statistical photon distribution of the radiation bath. If the field is in a Fock state $|n\rangle$ and the atom in an energy state $|+\rangle$ then the state of the entire system oscillates according to the Rabi frequency and depicts closed paths on the 2-sphere. The field in Glauber states leads to the collapses and revivals of the atomic population invertion that are well known in the literature. The reduced state of the atom, on the other hand, is just a mixed state and describes trajectories in the interior of the ball. In summary, we have analyzed here the geometry of the space state associated to a single qubit. The analysis of the case when the atom is in a mixed state as initial condition is going to be published elsewhere.

References

[1] Mielnik B., Geometry of quantum states, *Comm. Math. Phys.* **9** (1968) 55-80
[2] Mielnik B, Theory of filters, *Comm. Math. Phys.* **15** (1969) 1
[3] Mielnik B., Generalized quantum mechanics, *Comm. Math. Phys.* **37** (1974) 221
[4] Brody D.C. and Hughston L.P., Geometric quantum mechanics, *J. Geom. Phys.* **38** (2001) 19
[5] Mielnik B. and Rosas-Ortiz O., *Quantum Mechanical Laws*, in Fundamentals of Physics [Morán-López J.L. Ed.], Encyclopedia of Life Support Systems (EOLSS), Developed under the Auspices of the UNESCO, Eolss Publishers, Oxford, United Kingdom (2007/Rev. 2009)
[6] Mielnik B., Convex Geometry: A Travel to the Limits of Our Knowledge, in *Geometric Methods in Physics*, Springer Basel, 2013, p. 253
[7] Mielnik B., Evolution loops, *J. Math. Phys.* **27** (1986) 2290
[8] Fernández D. and Mielnik B., Controlling quantum motion, *J. Math. Phys.* **35** (1994) 2083
[9] Fernández D. and Rosas-Ortiz O., Inverse techniques and evolution of spin-1/2 systems, *Phys. Lett. A.* **236** (1997) 275
[10] Emmanouilidou A. and Zhao X.G., Steering an eigenstate to a destination, *Phys. Rev. Lett.* **85** (2000) 1626
[11] Fernández D. and Rosas-Ortiz O., Evolution loops and spin-1/2 systems, in *Coherent States, Quantization and Gravity*, Schlichenmaier M *et al* (Eds), Warsaw University Press 2001, p. 81
[12] Rosas-Ortiz O., Quantum control of two-level systems, *IOP Conf. Proc.* **185** (2004) 485
[13] Rezakhani A.T. and Zanardi P., General setting for a geometric phase of mixed states under an arbitrary non unitary evolution, *Phys. Rev. A* **73** (2006) 012107
[14] Enríquez-Flores M. and Rosas-Ortiz O., Atomic Schrödinger cat-like states, *AIP Conf. Proc.* **1287** (2010) 74
[15] Mielnik B., Quantum operations: technical or fundamental challenge?, e-print arXiv:1305.3664
[16] Bengtsson I. and Życzkowski K., *Geometry of Quantum States. An Introduction to Quantum Entanglement*, Cambridge University Press, 2006
[17] von Neumann J, *Mathematical foundations of quantum mechanics*, Princeton University Press, 1955
[18] Enríquez M. and Rosas-Ortiz O., The Kronecker product in terms of Hubbard operators and the Clebsch-Gordan decomposition of $SU(2) \times SU(2)$, *Ann. Phys.* **339** (2013) 218
[19] Thaller B., *Advanced Visual Quantum Mechanics*, Springer-Verlag, 2005
[20] Schlosshauer M., *Decoherence and the Quantum-to-Classical Transition*, Springer-Verlag, 2007
[21] Hopf H., Über die Abbildungen der dreidimensionalen Sphäre auf die Kugelfiche, *Math. Ann.* **104** (1931) 637
[22] Nakahara M., *Topology, Geometry and Physics*, IOP Publishing, 2003
[23] Enríquez M. and Rosas-Ortiz O., Spectral design to control the time-evolution of a two-level atom in single mode radiation fields, preprint Cinvestav (2013)
[24] Enríquez M. and Rosas-Ortiz O., Dynamics of two atoms in a double Jaynes-Cummings model, preprint Cinvestav (2013)
[25] Gerry C. and Knight P. L, *Introductory Quantum Optics*, Cambridge University Press, 2005
[26] Haroche S. and Raimond J. M., *Exploring the Quantum: Atoms, Cavities and Photons*, Oxford Graduate Texts, 2006
[27] Jaynes T. and Cummings F.W., Comparison of quantum and semiclassical radiation theories with application to the beam maser, *Proc. IEEE* **51** (1963) 89
[28] Gea-Banacloche J., A new look at the Jaynes-Cummings model for large fields: Bloch sphere evolution and detuning effects. *Optics communications* **88** (1992) 531